

Self-Assembled Monolayer of Cyclopentadienyl Ruthenium Thiolate Schiff Base-on-Gold, for Amperometric Detection of H₂O₂

Lawrence A. Ticha, Priscilla G.L. Baker, Hanna S. Abbo, Salam J.J. Titinchi, Emmanuel I. Iwuoha*

Department of Chemistry, University of the Western Cape, Robert Sobukwe Road, Bellville 7535, Cape Town, South Africa. Tel: +27 21 9593054

*E-mail: eiwuoha@uwc.ac.za

Received: 4 May 2014 / Accepted: 17 July 2014 / Published: 29 September 2014

A novel cyclopentadienylruthenium(II)thiolato Schiff base complex (Ru(II) thiolato complex), [Ru(SC₆H₄NC(H)C₆H₄O(CH₂)₂SMe)(η⁵-C₂H₅)]₂, was synthesized and deposited as a self assembled monolayer (SAM) on Au electrode using dichloromethane as the deposition solvent. The SAM's electroactivity was activated by cycling the electrode in 0.1 M NaOH from -200 mV to +600 mV before using it for electrochemical measurements. Quasi-reversibility of the SAM-modified Au electrode in CH₂Cl₂ containing tetrabutylammonium tetrafluoroborate (TBATFB) (0.1 M) was confirmed by anodic-to-cathodic CV peak ratio, $I_{p,a}/I_{p,c}$, value of 1.42 and peak separation, ΔE_p , value of 85 mV. Randles-Sevcik analysis of the CV data indicated a diffusion limited process. Horseradish peroxidase (HRP) was potentiostatically incorporated on the Au/SAM electrode at +700 mV vs. Ag/AgCl in phosphate buffer saline (PBS) (0.1 M phosphate and 2.7 mM KCl), pH 6.8. The resultant biosensor was used for the amperometric determination of H₂O₂ in PBS, pH 6.8. at +200 mV vs. Ag/AgCl. The electrode system gave a sensitivity of $5.11 \times 10^{-11} \mu\text{A mM}^{-1}$ and a detection limit of 5.26 mM for H₂O₂.

Keywords: Cyclopentadienylruthenium(II) thiolato Schiff base, Self-assembled monolayer, Horseradish peroxidase, Cyclic voltammetry, Amperometric biosensor.

1. INTRODUCTION

Amperometric biosensors have been used in versatile fields ranging from clinical diagnostics to environmental analysis and even to the detection of chemical and biological war-fares deleterious to human health. Amperometric biosensors are analytical devices or biosensing systems in which a biological component specifically recognizes the target analyte [1]. The immobilization of

biomolecules by using suitable electrochemical materials plays a crucial role in the construction of biosensors. Main strategies of biomolecule immobilisation include physical adsorption, cross-linking, covalent bonding, and entrapment in gels or membranes, amongst other techniques [2]. The term “Self-assembly” involves the arrangement of atoms and molecules into an ordered or even aggregate of functional entities without the intervention of mankind towards an energetically stable form. Self-assembled monolayer (SAM) formation induced by strong chemisorption between the substrate and head group of selected organic molecules provides one of the most elegant approaches towards making ultra thin organic film with controlled thickness [3]. One of the most widely used systems in SAM formation is the adsorption of sulphur derivatives (thiols, disulfides) on gold [4]. Self assembled monoayers of organosulfur compounds on gold electrodes are very promising for the construction of electrochemical biosensors. Exposure of a gold surface to a dilute solution (1.0 mM) of *n*-alkanethiol results in a chemisorbed monolayer that is densely packed in two dimensions and excludes ions and water from the underlying gold electrode [5,6,7]. The thermodynamically favourable formation of the gold-thiolate bond makes the gold-thiol system ideal for monolayer self assembly schemes, and the stability of that bond over a wide range of applied potential makes such a system suitable for electrochemical studies. Self assembly chemistry offers advantages over other approaches to electrode surface modification such as polymer films, which are usually much thicker and have considerable tertiary structure, and transferred Langmuir-Blgett (LB) films, which often contain many defects and can be intrinsically unstable. The main motivations behind the modification of the electrode surface are: (i) improved electrocatalysis (ii) freedom from surface fouling and (iii) prevention of undesirable reactions competing kinetically with the desired electrode process.

Peroxides pose a special threat to the environment. The detection and quantification of peroxides in the industrial effluent are carried out through volumetric, colorimetric and chemiluminescence techniques which are complex time consuming and are prone to interferences. Because of their high specificity, selectivity, rapid response and portability with user-friendly operational technology requiring minimal and no technical handling, amperometric biosensors are suitable alternatives. The hydrogen peroxide SAM-based nanobiosensor will provide a quicker alternative analytical procedure for the detection of peroxides. Furthermore, the biosensor will be in a single test-use format, thus avoiding the possibility of transducer fouling.

Horseradish peroxidase (HRP) is the most common peroxidase and probably the most studied member of the super family of heme containing plant peroxidases. Peroxidases catalyse the oxidation of various electron donor substrates (e.g. phenols, aromatic amines) with hydrogen peroxide [8]. By immobilising peroxidase on the SAM-derivatised Au electrode, the electrode system can substitute the electron donor substrate in the peroxidase reaction cycle. This process is usually referred to as direct electron transfer [9]. Peroxidase is oxidised by H₂O₂ and then subsequently reduced by electrons provided by the SAM on gold electrode. Peroxidase biosensors based on direct electron transfer are used for the detection of hydrogen peroxide and small organic hydroperoxides. Combined with H₂O₂ producing oxidases, they are also used for monitoring the concentration of oxidase substrates, e.g. glucose, alcohol, glutamate and choline [10].

In recent years, there has been considerable interest in transition metal complexes containing Schiff bases. These are popular ligands in coordination chemistry due to their ease of synthesis and

their ability to be readily modified both electronically and sterically. Mixed donor Schiff bases have been used extensively in catalysis. Most of the mixed-donor Schiff base ligands developed to date have nitrogen with phosphorous or oxygen atoms as the other donor unit. Little has been done on sulphur containing mixed-donor Schiff base ligands [11,12]. The fascinating electron-transfer and energy-transfer properties displayed by the complexes of ruthenium together with Schiff bases warrant their exploitation for application in electrocatalysis.

Ruthenium offers a wide range of oxidation states and the reactivity of the ruthenium complexes depend on the stability and inter-convertibility of these oxidation states, which in turn depend on the nature of ligands bound to the metal [13]. In this study the SAM of a novel cyclopentadienylruthenium(II) thiolato Schiff base complex modified with HRP, was prepared on a Au electrode and applied in the electro-catalytic reduction of H_2O_2 .

2. EXPERIMENTAL SECTION

2.1. Materials

4-Hydroxybenzaldehyde (98%), 2-chloroethylmethyl sulphide (97%), potassium carbonate, 4-aminothiophenol, bis(cyclopentadienyl)ruthenium(II) (97%), horseradish peroxidase (HRP, 1.10 U/mg, P6782), 30% (v/v) hydrogen peroxide solution and silica gel (230-400 mesh) were purchased from Sigma-Aldrich. All other reagents were of analytical grade and were used without further purification. Solvents were refluxed over an appropriate drying agent, distilled and degassed prior to use.

2.2. Instrumentation

All electrochemical analysis was performed with a bioanalytical systems electrochemical analyzer (BAS100/W) software using either CV) or OSWV. A conventional three electrode electrochemical cell was employed in the study used a gold working, Ag/AgCl reference and a platinum wire auxiliary electrodes. A negative oxidation current was used for the display of all figures. All cyclic voltammograms were carried out at a scan rate of 50 mV s^{-1} , unless otherwise stated. Square-wave voltammetry were carried out using a step potential of 4 mV, amplitude of 25 mV and a frequency of 15 Hz. The synthesis of $[\text{Ru}(\text{Cp})\text{thiolato}]_2$ complex and precursor materials were carried out under dry nitrogen by using a Schlenk line. Toluene and acetone were pre-dried, distilled and stored over 3 Å molecular sieves. $^1\text{H-NMR}$ spectra of the ligand were recorded at room temperature in CDCl_3 or DMSO-d^6 on a Varian Gemini 2000 instrument. Sample signals are relative to the resonance of residual protons on carbons in the solvent. The FT-IR measurements were carried out on a Perkin-Elmer Spectrum 100 FTIR spectrometer. Elemental analysis was performed by the micro analytical laboratory at the University of Cape Town, South Africa.

2.3. Buffers and solutions

All electrochemical experiments were carried out in phosphate buffer saline (PBS) (0.1 M phosphate and 2.7 mM KCl), pH 6.8. Deionised water (Milli-Q, Millipore, Japan) purification system was used to prepare electrolyte solutions. All experiments were carried out under argon atmosphere.

2.4. Synthesis

2.4.1. Synthesis of $\text{OHCC}_6\text{H}_4\text{O}(\text{CH}_2)_2\text{SMe}$ (a)

To a solution of 4-hydroxybenzaldehyde (1.0 g, 8.19 mmol) dissolved in acetone (50 mL) was added K_2CO_3 (5 g), followed by the addition of 2-chloroethylmethylsulphide (1.82 mL, 16.38 mmol). The reaction mixture was refluxed for 48 h at 55 °C under nitrogen atmosphere. Upon cooling to room temperature, a pale orange-yellow liquid was obtained, which was chromatographed on silica gel (230-400 mesh), CH_2Cl_2 :hexane (1:3) eluent to afford the pure compound with a yield of 1.42 g (88.3%).

$^1\text{H-NMR}$ (CDCl_3): δ 9.84(s, 1H, CHO) 7.82 (d, 2H, $J_{\text{HH}} = 8.8$ Hz, OHCC_6H_4), 6.98 (d, 2H, $J_{\text{HH}} = 8.6$ Hz, OC_6H_4), 4.27 (t, 2H, OCH_2), 2.88 (t, 2H, SCH_2), 2.22 (s, 3H, SCH_3).

2.4.2. Synthesis of $\text{HSC}_6\text{H}_4\text{NC}(\text{H})\text{C}_6\text{H}_4\text{O}(\text{CH}_2)_2\text{SMe}$ (b)

Compound (a) (0.5 mL, 2.71 mmol) and 4-aminothiophenol (0.34 g, 2.71 mmol) were dissolved in toluene (50 mL). After addition of a few drops of glacial acetic acid, the reaction mixture was stirred overnight under nitrogen for 18 h at room temperature. Evaporating the solvent under vacuum, yellow viscous oil was obtained. The product crystallized from CH_2Cl_2 :hexane (1:3) at -18 °C. After filtration, the solid was washed with hexane and dried in vacuum to afford a yellow solid. Yield = 0.39 g (47%).

$^1\text{H-NMR}$ (CDCl_3): δ 8.31 (s, 1H, $\text{C}(\text{H})=\text{N}$), 7.88 (d, 2H, $J_{\text{HH}} = 8.1$ Hz, $\text{C-C}_6\text{H}_4$), 7.2 (d, 2H, $J_{\text{HH}} = 8.4$ Hz, NC_6H_4), 7.11 (d, 2H, $J_{\text{HH}} = 8.1$ Hz, OC_6H_4), 7.00 (d, 2H, $J_{\text{HH}} = 8.5$ Hz, SC_6H_4), 4.22 (t, 2H, OCH_2), 2.93 (t, 2H, SCH_2), 2.13 (s, 2H, SCH_3). Anal. calcd. For $\text{C}_{16}\text{H}_{17}\text{NOS}_2$: C, 63.37; H, 5.61; N, 4.62%. Found: C, 63.54; H, 5.38; N, 4.31%. IR $\text{C}=\text{N}$ ($\nu = 1593$ cm^{-1}).

2.4.3. Synthesis of $[\text{Ru}(\text{SC}_6\text{H}_4\text{NC}(\text{H})\text{C}_6\text{H}_4\text{O}(\text{CH}_2)_2\text{SMe})(\eta^5\text{-C}_5\text{H}_5)]_2$, $\{[\text{Ru}(\text{Cp})\text{thiolato}]_2$ complex (where $\text{Cp} = \eta^5\text{-C}_5\text{H}_5$) (c)

To a suspension of bis(cyclopentadienyl)ruthenium(II) (0.051 g, 0.216 mmol) in toluene (50 mL) was added compound (b) (0.058 g, 0.216 mmol) which was stirred at room temperature for 24 h. A yellow solid was obtained, filtered, recrystallized from CH_2Cl_2 :hexane (1:3), washed repeatedly with hexane and dried in vacuum. A yellow solid was obtained. Yield = 0.022 g (44%).

$^1\text{H-NMR}$ (DMSO-d_6): δ 8.32 (s, 2H, $\text{C}(\text{H})=\text{N}$), 8.13 (d, 4H, $J_{\text{HH}} = 8.1$ Hz, $\text{C-C}_6\text{H}_4$), 7.82 (d, 4H, $J_{\text{HH}} = 8.1$ Hz, NC_6H_4), 7.02 (dd, 8H, SC_6H_4 and OC_6H_4), 4.51 (s, 10H, C_5H_5), 4.13 (t, 4H, OCH_2),

2.97(t, 4H, SCH₂), 2.21 (s, 6H, SCH₃). Anal. calcd. For C₄₂H₄₂N₂O₂S₄Ru₂: C, 53.85; H, 4.49; N, 2.99%. Found: C, 54.11; H, 4.15; N, 2.06%. IR C=N ($\nu = 1596 \text{ cm}^{-1}$).

2.5. Immobilisation Procedures

2.5.1. Immobilisation of cyclopentadienylruthenium(II) thiolato Schiff base on gold

Before the formation of the [Ru(Cp)thiolato]₂ complex self-assembled monolayer (SAM) on top of the gold electrode, a pre-treatment procedure based on the work of Willner and Rinklin [14] and Schlereth *et al.* [15] was applied to the gold electrode. A 3 mm diameter gold disk was polished progressively with 15, 3 and 1 μm diamond powder (BAS MF-2059) for 1 min in each case. The electrode was rinsed and sonicated in deionised water for 5 min. It was then immersed for 1 h in hot 2 M KOH solution and for 10 min in concentrated solutions of HNO₃ and H₂SO₄ while rinsing with deionised water after each immersion. The pre-treated Au was rinsed with CH₂Cl₂ and placed in 1 mM [Ru(Cp)thiolato]₂ complex for 24 h at ambient temperature during which [Ru(Cp)thiolato]₂ complex self-assembled monolayer (SAM) was formed on the AuE. The SAM-modified electrode was rinsed with copious amount of CH₂Cl₂, and preconditioned for electrochemical studies by performing CV in 0.1 M NaOH using a potential window of -200 mV to -600 mV vs. Ag/AgCl at 50 mV s⁻¹.

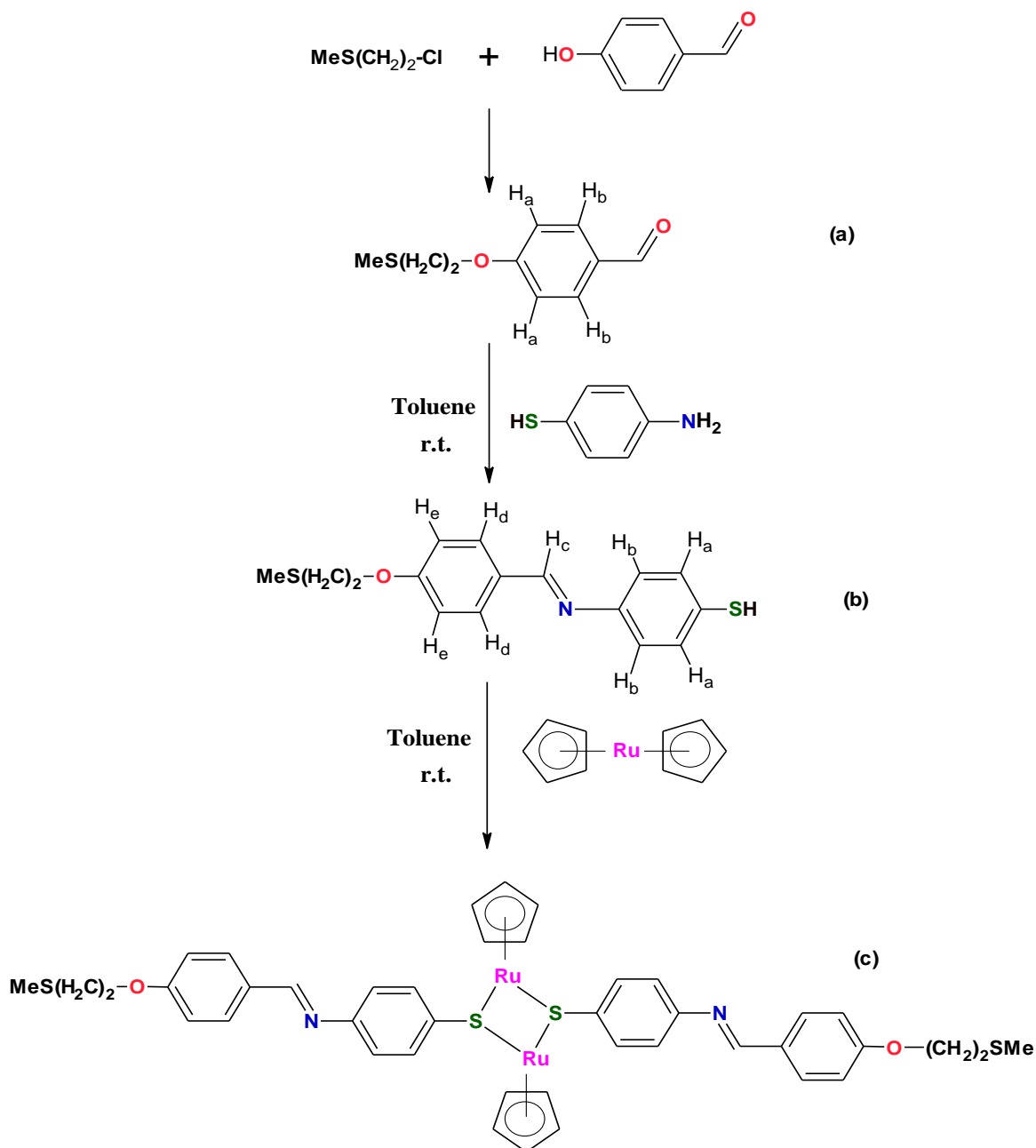
2.5.2. Immobilisation of HRP on SAM

The Au/SAM electrode was oxidised in 1 mL PBS, pH 6.8 containing 1 mg mL⁻¹ HRP at +700 mV vs. Ag/AgCl for 1500 s. During this potentiostatic oxidation process, the enzyme became electrostatically attached to the SAM surface. The enzyme solution was carefully recovered from the cell and stored at 4 °C for re-use.

3. RESULTS AND DISCUSSION

3.1. Synthesis and characterisation

The *para*-alkoxybenzaldehyde used for the preparation of the Schiff base ligand was prepared by the Williamson reaction (Scheme 1, compound a). This was achieved by the reaction of 2-chloroethylmethylsulphide and 4-hydroxybenzaldehyde in refluxing acetone.



Scheme 1. Reaction scheme for the preparation of $[\text{Ru}(\text{Cp})\text{thiolato}]_2$ complex.

Improved yield was achieved by the use of finely ground potassium carbonate; otherwise the yield of the alkoxybenzaldehyde was low. Trace amounts of a by-product formed from the deprotonation of the carbonyl group were present as could be seen from the $^1\text{H-NMR}$ of the crude product, but the by-product was easily separated from the product by column chromatography using silica gel and CH_2Cl_2 :hexane (1:3) as eluent to give an analytically pure product. The difference in our synthetic protocol and that reported in literature; where potassium carbonate was used is in the choice of solvent. Binnemans *et al.* used butanone [16], while Scamporrino *et al.* used a mixture of toluene and water [17]. Other reported reaction conditions used potassium hydroxide in DMF or ArSO_2Cl and

phenol in ethanol:water (1:1) mixture [18,19]. In the above literature procedures the yields were in the range of 75-95%, while moderate yield was achieved using our synthetic method.

The $^1\text{H-NMR}$ of the analytically pure (compound a) showed a prominent peak due to the hydrogen of the CHO group at 9.84 ppm which is typical of benzaldehyde derivatives. In addition, there were two sets of doublets at 6.98 ppm and 7.82 ppm due to the H_a and H_b protons respectively. The signal of the H_b proton is expected to be up-field because of the shielding effect of the alkoxy chain while H_a is expected to be downfield because of the electron withdrawing nature of the carbonyl group. The simplicity in assigning the H_a and H_b is helpful to allocate the peaks of Schiff base compound produced from the reaction of alkoxybenzaldehyde with 4-aminothiophenol. The alkyl chain in the pure product gave triplets at 2.88 and 4.10 ppm due to the higher electron withdrawing nature of oxygen over sulphur ($-\text{OCH}_2\text{CH}_2-\text{S}-$). A singlet at 2.19 ppm was unambiguously assigned to the terminal methyl group ($-\text{CH}_3$).

The Schiff base ligand was prepared by condensation of equimolar amounts of 4-aminothiophenol and the prepared alkoxybenzaldehyde. FT-IR spectrum of the ligand shows the appearance of an imine peak at 1592 cm^{-1} and the disappearance of the carbonyl peak in the aldehyde (1730 cm^{-1}) which confirm the formation of imine group. The presence of the imine group was further confirmed by $^1\text{H-NMR}$ which observed at 8.39 ppm, comparable to similar compounds [20]. In similar Schiff base compounds ($4\text{-H}_{2n+1}\text{C}_n\text{OC}_6\text{H}_4\text{NC(H)C}_6\text{H}_4\text{OC}_n\text{H}_{2n+1}\text{-4}$), where alkyl chains replaced the thiols, the imine proton signals were found at 8.50 ppm [21], indicating that the effect of substituent on the chemical shift is generally minimal [22]. The rest of the chemical shifts helped in identifying the products. The general pattern of the $^1\text{H-NMR}$ in the aromatic region consisted of four sets of doublets which are typical AB type patterns for the four protons of the two phenyl rings. The most up-field doublet was due to H_a (6.98 ppm) with the next doublet at 7.24 ppm due to H_e . All other signals were typical of thiol and alkyl functional groups. The resonance signal for the S-H proton at 3.52 ppm is similar to that of organic thiols at 3.45 - 3.48 ppm [23].

The Schiff base complex was synthesised by reacting equimolar of thiol-imine ligand (b) with bis(cyclopentadienyl)ruthenium(II) (Scheme 1) in moderate yield (44%). The complex was found to be remarkably stable to air and moisture at room temperature for several weeks. Spectroscopic characterization and elemental analyses of the ligand and the complex confirmed the products as formulated in Scheme 1. The C=N stretching frequency did not shift during complexation, which confirms that complexation did not occur through nitrogen of azomethine group. The $^1\text{H-NMR}$ spectrum of the bimetallic ruthenium complex is a typical of cyclopentadienyl thiolato analogue complexes [24].

The main NMR-spectroscopic feature of the complex is the observation of a new singlet at 4.51 ppm which is assigned to cyclopentadienyl ring protons. On the other hand, $^1\text{H-NMR}$ spectral data showed that thiolato resonance of the complexes and that of free ligands were very similar, particularly the chemical shift for the N=CH proton. Each of the two phenyl groups in the thiolato ligands of the complexes exhibit a classical AA'BB' spin system [25] in the ^1H NMR spectra. Further characterization of the complex was achieved by electrochemical methods (vide infra).

3.2. Electrochemical characterisation of [Ru(Cp)thiolato]₂ complex in solution

The nickel analogue of the Schiff base complexes, [Ni(SC₆H₄NC(H)C₆H₄OC_nH_{2n+1})(η⁵-C₂H₅)₂], (n = 4, 14, and 16) exhibit ideal reversible electrochemistry, offering low positive potential values vs. the normal hydrogen electrode (NHE) [26]. This paves the way for investigating them for possible applications as electron transfer mediators in biosensors. The intention of this study is to attempt is to expand this notion to a novel cyclopentadienylruthenium(II) thiolato Schiff base complex. Taking advantage of the π-back-bonding capability of ruthenium(II) and its accessibility in various oxidation states together with singular properties offered by the Schiff base ligands (ease of synthesis, versatility and their planarity) [26], a [Ru(Cp)thiolato]₂ complex was synthesized for the formation of a novel SAM on gold. The redox properties of this complex were investigated under stationary conditions at a gold electrode under argon “blanket”. Cyclic voltammetry in CH₂Cl₂ containing tetrabutylammonium tetrafluoroborate (TBATFB) (0.1 M) was used to interrogate the redox activity of this complex owing to its high sensitivity and reproducibility. Dilute concentrations of the complex (2 mM) were employed in all the voltammetric experiments. SAM formation using a very dilute solution gives ordered monolayer whereas a high concentration and long time (6 days) favour multiple layer formation [2]. The CV of the SAM (Figs 1a and 1b) displayed a well-defined wave assigned to the Ru^{III}/Ru^{II} redox couple. This process is observed with characteristics of high quasi-reversibility [27]. The peak separation, $\Delta E_p = (E_{p,a} - E_{p,c})$, formal potential, E° , peak current ratio, $(I_{p,a}/I_{p,c})$ values of 100 mV, 174 mV and 1.42, respectively, further attest to the quasi-reversibility of the complex (Fig. 1).

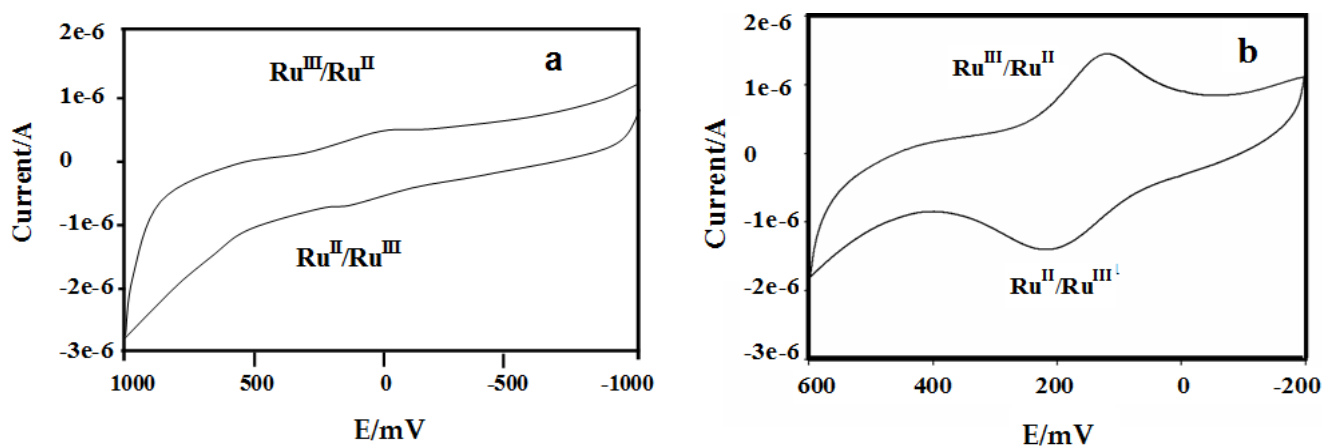


Figure 1. Cyclic voltammogram for 2 mM [Ru(Cp)thiolato]₂ complex on a bare gold electrode in CH₂Cl₂ containing 0.1 M TBATFB at a scan rate 50 mV s⁻¹.

Sweeping the electrode through potentials outside its potential window can deteriorate the behaviour of the system, due to the formation oxides or hydrogen evolution at the working electrode. The purpose of sweeping the potential over a wide range was to investigate the electrochemistry of the complex (Fig. 1a). It is clear that the Ru^{III}/Ru^{II} redox electrochemistry was the only redox activity present in the complex.

Figure 2 represents the Randels-Sevcik plot of the anodic peak currents of the $\text{Ru}^{\text{III}}/\text{Ru}^{\text{II}}$ redox couple. The plot was normalized to correct for double layer-charging. The near superimposition of the plots demonstrated the quasi-reversibility of the $\text{Ru}^{\text{III}}/\text{Ru}^{\text{II}}$ couple. Peak current was proportional to $\nu^{-1/2}$ ($r^2 = 0.98$) indicating electron diffusion limited response of the Au//SAM electrode, and ΔE_p did not change with varying scan rates. Further evidence for quasi-reversibility of the complex lie in the fact that the peak potential difference (ΔE_p) is 100 mV, with anodic to cathodic peak current ratio of 1.42 (Fig. 1b). However, the non-zero intercept may be attributed to non-faradaic currents, i.e. the complex is considered to be quasi-reversible [2]. Due to the Ru(II) thiolato Schiff base's strong redox properties, together with its methyl sulfide end-group, the complex was further investigated for its possible application as an electroanalytical self-assembled monolayer (SAM).

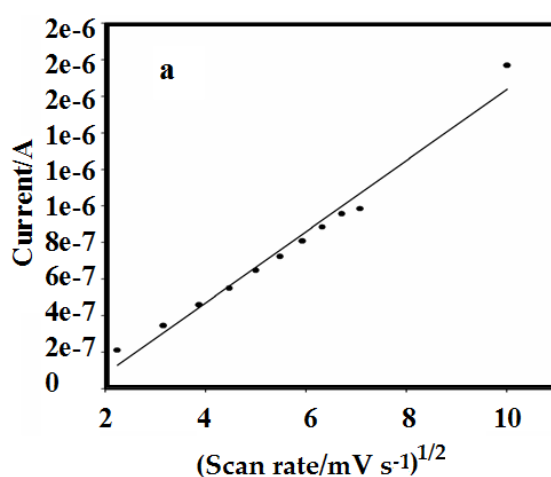


Figure 2. (a) Randels-Sevcik plot of the anodic peak currents of the CV of Au/SAM electrode performed at the scan rates 5 – 300 mV s^{-1} in CH_2Cl_2 containing 0.1 M TBATFB.

3.3. Characterization of $[\text{Ru}(\text{Cp})\text{thiolato}]_2$ complex on gold

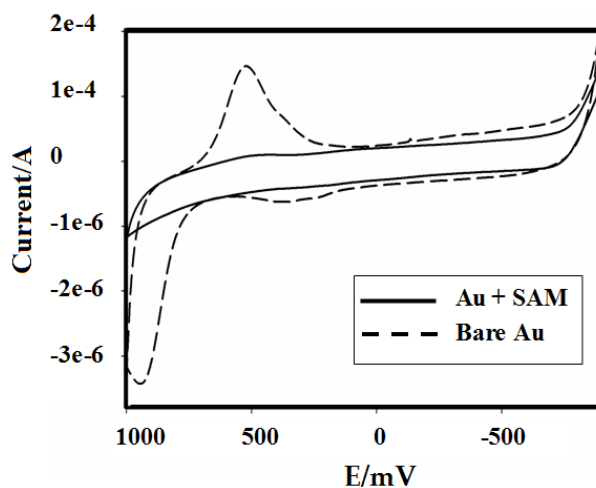


Figure 3. Cyclic voltammograms of bare Au and Au/SAM in PBS containing 2 mM ferricyanide as the redox probe.

In order to access the self-assembled monolayer formation on gold, the electrochemistry was studied in PBS containing 1 mM ferricyanide as the redox probe. The redox behaviour of this probe was completely inhibited following monolayer formation. Any redox activity observed for the Au/SAM is mainly due to the SAM deposition on gold electrode as indicated by a complete suppression of the oxygen redox peak of the probe as shown in Fig. 3 [20,27].

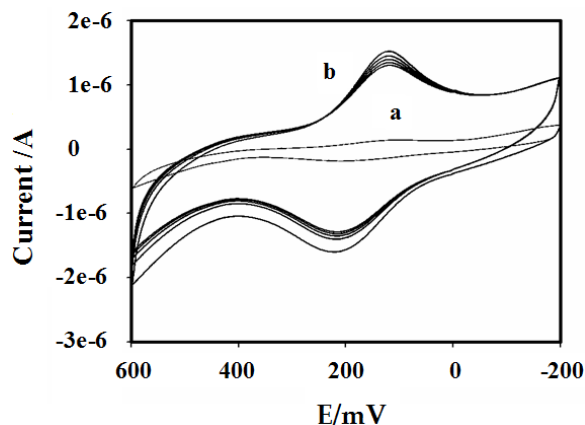


Figure 4. Cyclic voltammograms of SAM-modified Au electrode in PBS, pH 6.8 at 50 mV s^{-1} : (a) before NaOH-treatment and (b) 5 CV cycles after NaOH-treatment.

The thiol end-groups of the complex were protected by a methyl group to avoid oxidative S-S coupling [21]. The $[\text{Ru}(\text{Cp})\text{thiolato}]_2$ complex SAM required voltammetric cycling in base (0.1 M NaOH) from -200 to $+600 \text{ mV}$ ($v = 50 \text{ mV s}^{-1}$) to activate its electroactivity as demonstrated in Fig.4. Before cycling in base, the SAM showed minor redox activity but after treatment with NaOH a set of quasi-reversible peaks were clearly observed. As the number of cycles was increased, the areas under the anodic and cathodic peaks began to increase, reaching stability after 5 cycles (Fig. 4). This implies that the number of redox active molecules on the surface of the gold electrode has been increased. It could be explained that the desired cleavage of sulphur-methyl bond did not occur during the time in which the Au electrode was left standing in the deposition solution. In spite of the formation of SAM, the complex bounded weakly to the Au electrode via the lone pair donated by the thiol end groups. This justifies the initially observed poor electronic communication between the Ru(II) redox centres and the Au electrode. Continued cycling after stability will inevitably change the conformation of the SAM as a consequence of in-situ generation of covalent bonding between the sulphur and Au to form true SAM. This improved the electronic communication between the Ru(II) centres of the complex due to induced covalent bonding. Using NH_4OH and NaOH have also been exploited to a greater extent in deprotonating the alkyl end groups to minimise S-S bond formation, while using $(n\text{-C}_3\text{H}_7)_2\text{NH}$ or dimethylaminopyridine were found to be less effective in deprotonating the thiol end groups [28,29]. The deprotonation was achieved by adding small amounts of the base to the SAM deposition solution; so that the deprotonation takes place in bulk solution leaving the thiol end groups free to attach to the gold substrate for conventional self-assembly. In this work, deprotonation of SAM was done after its removal from the deposition solution. Figure 4 demonstrates this clearly as no electronic

communication was observed before cycling in 0.1 M NaOH. A close-packed SAM will block Faradaic processes from the electrode surface. Film ion barrier factor, Γ_{ibf} , was evaluated from charge produced by cycling the bare and the SAM-modified electrodes in 0.1 M NaOH solution (Fig. 4) according to equation 1.

$$\Gamma_{\text{ibf}} = 1 - Q_{\text{SAM}}/Q_{\text{Bare}} \quad (1)$$

where Q_{SAM} and Q_{Bare} are the charges under the gold oxide stripping peaks for SAM modified and bare gold electrode, respectively. It can be inferred from Figure 4 that non-detection of charge on the Au electrode after the deposition of $[\text{Ru}(\text{Cp})\text{thiolato}]_2$ Schiff base complex, indicates that the gold surface was completely isolated from the aqueous solution, which is the source of gold oxide formation [25].

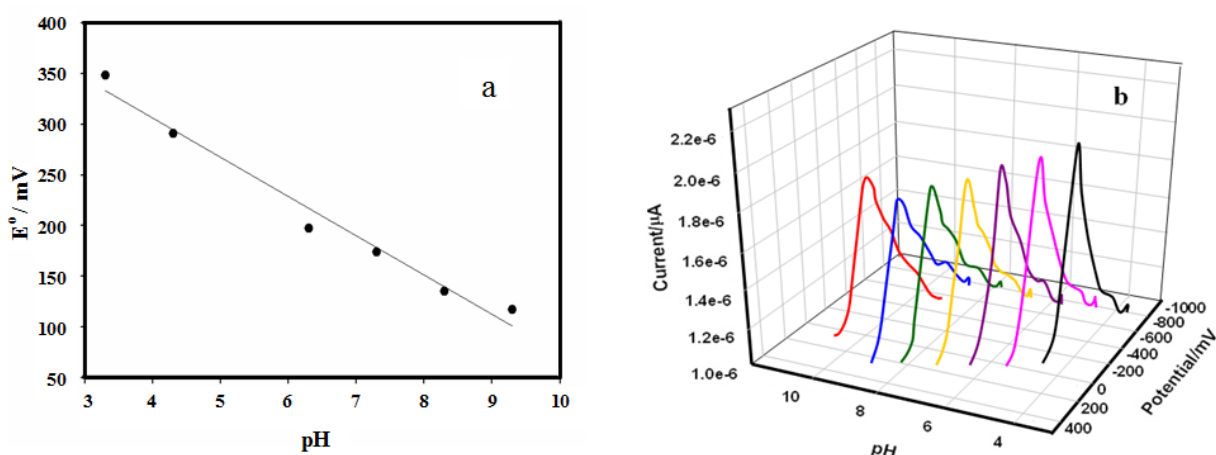
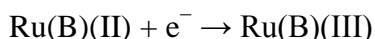
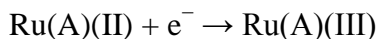


Figure 5. (a) The pH dependence of the formal potential of Au/SAM in PBS at scan rate of 50 mV s^{-1} , for pH 3.3 - 9.3; with a slope of -34 mV pH^{-1} demonstrating a two-electron, one-proton redox process. (b) The pH profile of the OSWV of Au/SAM in PBS at a scan rate of 50 mV s^{-1} .

Since no charge could be detected for the gold surface after deposition, Γ_{ibf} must be approximately unity, indicating that the SAM acts as a barrier against the permeation of electrolyte species. The ΔE_p value of the redox probe couple was 89.2 mV and the $I_{p,c}/I_{p,a}$ ratio was 1.26. These are pointers to the SAM's ability to mediate electron transfer reaction of any redox couple present in solution. Furthermore, to ascertain that the SAM layer was the only source of redox activity being observed, the $I_{p,a}$ was directly proportional to the scan rate, ν , which is consistent with what is expected for an electrochemical reaction involving a surface confined species that is uniformly distributed and non-interacting redox centres position at the same distance from the surface of the electrode. Deviation from ideal behaviour was attributed to either the non-uniformity of the distribution centres with respect to their distances to the electrode surface, and possible interactions like electrostatic repulsion or the irreversibility of the charge transfer processes involved. The formal potential of the SAM-modified electrode varied with pH (evaluated using OSWV in 0.1 M phosphate) is shown in Fig. 5b, with a

slope of about -34 over a pH range of 3.3 to 9.3 (Fig.5a). This is quite close to the theoretical value of -29 for a two-electron-one-proton redox process [4]. This is in agreement with Tafel analysis for the deduction of the number of electrons transferred for $[\text{Ru}(\text{SC}_6\text{H}_4\text{NC}(\text{H})\text{C}_6\text{H}_4\text{OC}_n\text{H}_{2n+1})(\eta^5\text{-C}_2\text{H}_5)_2]$, ($n = 4, 14, \text{ and } 16$) in bulk solution of CH_2Cl_2 containing 0.1 M TBATFB [26]. All Tafel plots gave values of approximately 2 for the number of electrons transferred as there are two Ru(II) centres per molecule, thus the reaction;



A similar observation has been reported by Ozoemena and Nyokong [30] for an iron phthalocyanine immobilized on a gold electrode. This can be attributed to water (in acidic or neutral medium), and hydroxyl group (in alkaline medium) coordinating to the Ru(II) centre. In this work, the chosen pH was close to neutral since an enzyme is used and enzymes are pH sensitive.

The calculated surface concentration, Γ , of the ruthenium redox centres is $1.591 \times 10^{-11} \text{ mol cm}^{-2}$ for the two electrons transferred, which is comparable to literature values [30,31]. It can be concluded that this monolayer is effectively non-permeable to electrolyte species (implying that the surface coverage is relatively pin-hole free) which led to the presumption that not all the Ru(II) groups attached to the surface of the gold electrode are electroactive. A possible reason is that all the methyl end groups were not removed during voltammetric cycling in NaOH, hence electronic communication between all the molecules and the electrode surface could not occur.

3.4. Hydrogen peroxide (H_2O_2) detection at the Au/SAM/HRP electrode

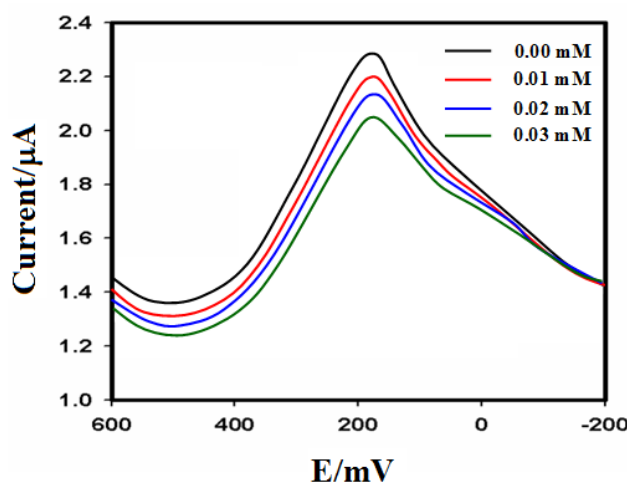


Figure 6. Anodic OSWV responses of Au/SAM/HRP in PBS, pH 6.8 to H_2O_2 .

Amperometric biosensors have been developed with electroactive polymers that can mediate electron transfer between enzyme active site and electrode surface [32-35]. In this study, horseradish

peroxidase (HRP), a heme-containing glycoprotein, was used as a model enzyme for catalytic reduction of H_2O_2 . The current is produced by the electrochemical reduction of HRP^{I} and HRP^{II} , which are two and one oxidation states higher than the native HRP resting state, respectively. The current should directly proportional to the concentration of H_2O_2 and used a basis for amperometric detection of H_2O_2 . HRP was electrostatically attached [36-37] to the SAM surface by applying anodic potential in the presence of HRP (1 mg mL^{-1}). Figure 6 depicts the square-wave voltammograms of the Au/SAM/HRP electrode in PBS, pH 6.8 in the presence H_2O_2 under anaerobic conditions.

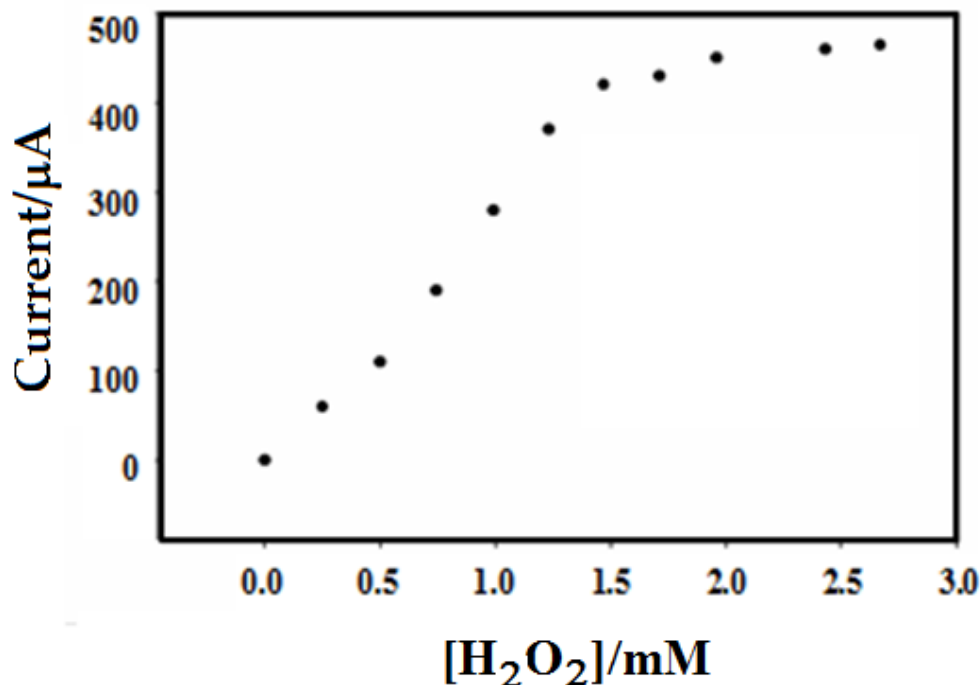


Figure 7. The H_2O_2 response curve of Au/SAM/HRP at +200 mV vs. Ag/AgCl in PBS, pH 6.8.

To ascertain that Ru(II) alone could not reduce H_2O_2 , CVs were performed on an HRP free SAM surface before and after the addition of H_2O_2 . Little change was observed in the cathodic peak currents. Therefore, HRP is playing a vital role in the reduction of H_2O_2 . The reduction processes proceeds by the conversion of HRP^{II} to HRP via a two electron reduction. The oxidised form of the redox compound is reduced at the electrode which is held at a constant suitable potential. The magnitude of the reduction current produced by the electrode reaction depends on the bulk concentration of the substrate. The normal practice has been to incorporate an electron transfer mediator in the biosensor film or reaction solution. Hence the electroactive self-assembled monolayer, (SAM) is used here as the mediator in the reagent less peroxide biosensor. Figure 7 represents the H_2O_2 response curve of Au/SAM/HRP biosensor at +200 mV. The sensor exhibited Michaelis-Menten kinetics. The detection limit (5.26 mM) was evaluated based on a signal-to-noise level of 3 and a sensitivity of $5.11 \times 10^{-11} \text{ } \mu\text{A mM}^{-1}$, demonstrating the potential application of the Au/SAM/HRP in the amperometric analysis of H_2O_2 . Although this novel approach has not yet reached lower detection

limits, with the advantages of SAM over other approaches for electrode surface fictionalization (ease of preparation and versatility), this approach is very promising for electrocatalytic reduction and analysis of H₂O₂. This technique can be improved by increasing the electroactive nature of Ru(II) molecules and by optimising enzyme catalysis parameters such as loading time on the SAM surface, pH and adaptation to a flow system, amongst others.

4. CONCLUSIONS

Structural analysis confirmed that a novel SAM of [Ru(Cp)thiolato]₂ Schiff base complex was successfully prepared and its electrochemistry was evaluated by CV and OSWV voltammetric techniques. Effective electronic communication between the Ru(II) metal centres was achieved by voltammetric cycling in 0.1 M NaOH. Scanning in alkaline medium removed the methyl end groups of the complex as evident from an increment in the redox peaks with increasing number of scans. The monolayer produced by the self-assembly of [Ru(Cp)thiolato]₂ complex allows tremendous flexibility to several applications depending upon their terminal functionalities (hydrophobic or hydrophilic) or by varying the chain length (distance control). The SAM exhibited a quasi-reversible electrochemistry which was attributed to the non-uniformity of the SAM monolayer or molecular interactions between the SAM molecules themselves. The electrocatalytic reduction of H₂O₂ at the Au/SAM/HRP was established by CV and OSWV, which revealed that the [Ru(Cp)thiolato]₂ complex effectively mediated electron transfer between the enzyme and the Au electrode. Altering the surface using a mixed monolayer approach, or by alteration of the complex itself, could improve the performance parameters of this novel [Ru(Cp)thiolato]₂ complex/peroxidase-based biosensor.

ACKNOWLEDGEMENTS

The authors would like to acknowledge the National Research Foundation (NRF) of South Africa for research grants.

References

1. (a) S. Xu, G. Tu, B. Peng and X. Han, *Anal. Chim. Acta*, 570 (2006) 151; (b) C.T. Nguyen, T. H. Tran, X. Lub and R.M. Kasi, *Polym. Chem.*, 5 (2014) 2774.
2. (a) N.K. Chaki and K. Vijayamohanan, *Biosens. Bioelectron.*, 17 (2002) 1; (b) M. Trojanowicz, *Electrochem. Commun.*, 38 (2014) 47.
3. (a) K. Sun, B. Jiang and X. Jiang, *J. Electroanal. Chem.*, 656 (2011) 223; (b) Y. Sato, M. Fujita, F. Mizutani and K. Uosaki, *J. Electroanal. Chem.*, 409 (1996) 145.
4. (a) M.D. Porter, T.B. Bright, D.L. Allara and C.E.D. Chidsey, *J. Am. Chem. Soc.*, 109 (1987) 3559; (b) A.L. Eckermann, D.J. Feld, J.A. Shaw and T.J. Meade, *Coord. Chem. Rev.*, 254 (2010) 1769; (c) A. Mishra, C.-Q. Ma and P. Bäuerle, *Chem. Rev.*, 109 (2009) 1141; (d) J.C. Love, L.A. Estroff, J.K. Kriebel, R.G. Nuzzo and G.M. Whitesides, *Chem. Rev.*, 105 (2005) 1103.
5. H.O. Finklea, S. Avery, M. Lynch and T. Furtch, *Langmuir*, 3 (1987) 409.
6. A. Lindgren, T. Ruzgas, L. Gorton, E. Csoregi, G. Bautista Ardila, I.Y. Sakharov and I.G. Gazaryan, *Biosens. Bioelectron.*, 15 (2000) 491.

7. C. Vericat, M.E. Vela, G. Benitez, P. Carro and R. C. Salvarezza, *Chem. Soc. Rev.*, 39 (2010) 1805.
8. A.L. Ghindilis, P. Atanasov and E. Wilkins, *Electroanalysis* 9 (1997) 661.
9. S. Ray, S. Chand, Y. Zhang, S. Nussbaum, K. Rajeshwar and R. Perera, *Electrochim. Acta*, 99 (2013) 85.
10. P.N. Mashazi, K.I. Ozoemena and T. Nyokong, *Electrochim. Acta*, 52 (2006) 177; D.P. Halbach and C.G. Hamaker, *J. Organomet. Chem.*, 691 (2006) 3349.
11. K.P. Balasubramanian, K. Parameswari, V. Chinnusamy, R. Prabhakaran and K. Natarajan, *Spect. Chim. Acta A*, 65 (2006) 678.
12. (a) F. Basuli, D. A. Kumar, G. Mostafa. S.-M. Peng and S. Bhattacharya, *Polyhydron*, 19 (2000) 1663; (b) K. Nakajima, S. Ishibashi, M. Inamo and M. Kojima, *Inorg. Chim. Acta*, 325 (2001) 36; (c) K. Nakajima, Y. Ando, H. Mano and M. Kojima, *Inorg. Chim. Acta*, 274 (1998) 184.
13. P.M.S. Monk, *Fundamentals of Electroanalytical Chemistry*, Wiley, NY 2001.
14. I. Willner and A. Riklin, *Anal. Chem.* 66 (1994) 1535.
15. D.D. Schlereth, E. Katz and H.-L. Schmidt, *Electroanalysis*, 7 (1995) 46.
16. K. Binnemans, Y. G. Galyametdinov, S. R. Collinson and D. W. Bruce, *J. Matter. Chem.*, 8 (1998) 1551.
17. E. Scamporrino, D. Vitalini and P. Mineo, *Macromolecules*, 32 (1999) 4247.
18. B. Bilgin-Eran, C. Yorur and S. Uzman, *J. Organomet. Chem.*, 655 (2002) 105.
19. Z.-F. Li, C.-F. Ning, S.-J. Zhang, S.-Y. Zhang, S. Cao, D. Zhang and Q.-F. Zhou, *Macromolecules*, 32 (1999) 7040.
20. (a) A. Morrin, R.M. Moutloali, A.J. Killard, M.R. Smyth, J. Darkwa and E.I. Iwuoha, *Talanta* 64 (2004) 30; (b) F.A. Nevondo, A.M. Crouch and J. Darkwa, *J. Chem. Soc. Dalton Trans.*, (2000) 43; (c) J. Darkwa, R.M. Moutloali and T. Nyokong, *J. Organomet. Chem.*, 564 (1998) 37.
21. A. Houlton, N. Jasim, R.M.G. Roberts, J. Silver, D. Cunningham, P. McArdle and T. Higgins, *J. Chem. Soc. Dalton Trans.*, (1992) 2235.
22. X. Yang, C.L. Stern and T.J. Marks, *J. Am. Chem. Soc.*, 116 (1994) 10015.
23. R.M. Moutloali, J. Bacsá, W.A. Ddamba and J. Darkwa, *J. Organomet. Chem.*, 629 (2001) 171.
24. H. Friebolin, *Basic one- and two-dimensional NMR spectroscopy*, VCH, New York, 2nd edition 1993, p. 121.
25. R.M. Moutloali, F.A. Nevondo, J. Darkwa, E.I. Iwuoha and W. Henderson, *J. Organomet. Chem.*, 656 (2002) 262.
26. H.H. Girault, *Analytical and Physical Electrochemistry*, Taylor & Francis 2004.
27. S.O. Pinheiro, J.R. de Sousa, M.O. Santiago, I.M.M. Carvalho, A.L.R. Silva, A.A. Batista, E.E. Castellano, I.S. Moreira, J. Ellena, I.S. Moreira and I.C.N. Diogenes, *Inorg. Chim. Acta*, 359 (2006) 391.
28. S. Campuzano, R. Galvez, M. Pedrero, F.J. Manuel de Villena and J.M. Pingarron, *J. Electroanal. Chem.*, 526 (2002) 92.
29. J.M. Tour, L. Jones, D.L. Pearson, J.J.S. Lamba, T.P. Burgin, G.M. Whitesides, D.L. Allara, A.N. Parikh and S. Atre, *J. Am. Chem. Soc.*, 117 (1995) 9529.
30. K. Ozoemena and T. Nyokong, *Electrochim. Acta* 47 (2002) 4035.
31. J. Li, J. Yan, Q. Deng, G. Cheng and S. Dong, *Electrochim. Acta*, 42 (1997) 961.
32. R.F. Ajayi, U. Sidwaba, U. Feleni, S.F. Douman, O. Tovide, S. Botha, P. Baker, X.G. Fuku, S. Hamid, T.T. Waryo, S. Vilakazi, R. Tshikhudo and E.I. Iwuoha, *Electrochim. Acta*, 128 (2014) 149.
33. C.E. Sunday, M. Bilibana, S. Qakala, O. Tovide, K. M. Molapo, G. Fomo, C. O. Ikpo, T. Waryo, G. Mbambisa, B. Mpushe, A. Williams, P.G.L. Baker, S. Vilakazi, R. Tshikhudo and E. I. Iwuoha, *Electrochim. Acta*, 128 (2014) 128.

34. O. Tovidé, N. Jaheed, N. Mohamed, E. Nxusani, C.E. Sunday, A. Tsegaye, R.F. Ajayi, N. Njomo, H. Makelane, M. Bilibana, P.G. Baker, A. Williams, S. Vilakazi, R. Tshikhudo and E.I. Iwuoha, *Electrochim. Acta*, 128 (2014) 138.
35. J.C. Kemmegne-Mbouguen, E. Ngameni, P.G. Baker, T. Waryo, B. Kgarebe and E. Iwuoha, *Inter. J. Electrochem. Sci.*, 9 (2014) 478.
36. A. Morrin, A. Guzman, A.J. Killard, J.M. Pingarron and M.R. Smyth, *Biosens. Bioelectron.*, 18 (2003) 715.
37. E.I. Iwuoha, D.S. de Villaverde, N.P. Garcia, M.R. Smyth and J.M. Pingarron, *Biosens. Bioelectron.*, 12 (1997) 749.

© 2014 The Authors. Published by ESG (www.electrochemsci.org). This article is an open access article distributed under the terms and conditions of the Creative Commons Attribution license (<http://creativecommons.org/licenses/by/4.0/>).